Parathyroid Hormone Hormone-Related Protein and the PTH Receptor Regulate Angiogenesis of the Skin

A. Godwin Diamond[1], Ryan M. Gonterman[1], Aileen L. Anderson[1], Keshav Menon[1], Carlos D. Offutt[1], Chad H. Weaver[1], William M. Philbrick[2] and John Foley[1,3,4]

In developing organs, parathyroid hormone (PTH)/parathyroid hormone-related protein (PTHrP) receptor (PPR) signaling inhibits proliferation and differentiation of mesenchyme-derived cell types resulting in control of morphogenic events. Previous studies using PPR agonists and antagonists as well as transgenic overexpression of the PPR ligand PTHrP have suggested that this ligand receptor combination might regulate the anagen to catagen transition of the hair cycle. To further understand the precise role of PTHrP and the PPR in the hair cycle, we have evaluated hair growth in the traditional K14-PTHrP (KrP) and an inducible bitransgenic PTHrP mice. High levels of PTHrP trangene expression limited to the adult hair cycle resulted in the production of shorter hair shafts. Morphometric analysis indicated that reduced proliferation in the matrix preceded the appearance of thinner hair follicles and shafts during late anagen. CD31 staining revealed that the late anagen hair follicles of the KrP mice were surrounded by reduced numbers of smaller diameter capillaries as compared to controls. Moreover, the fetal skins of the PTHrP and PPR knockouts (KOs) had reciprocal increases in the length, diameter, and density of capillaries. Finally, crossing the KrP transgene onto a thrombospondin-1 KO background reversed the vascular changes as well as the delayed catagen exhibited by these mice. Taken together, these findings suggest that PTHrP's influence on the hair cycle is mediated in part by its effects on angiogenesis.

Journal of Investigative Dermatology (2006) **126,** 2127–2134. doi:10.1038/sj.jid.5700338; published online 4 May 2006

INTRODUCTION

Parathyroid hormone-related protein (PTHrP) was initially identified in association with the paraneoplastic syndrome, humoral hypercalcemia of malignancy. This syndrome is produced when the tumor-derived amino (N)-terminal containing PTHrP peptides enter the circulation and stimulate the PTH/PTHrP receptor (PPR) in bone and kidney (Firkin *et al.*, 1996). The PPR is a G-protein-coupled receptor capable of signaling through both the adenyl-cyclase and phospho-lipase C second messenger pathways (Gardella and Juppner, 2001). PTHrP–PPR signaling regulates the development of several organ systems including the long bone, tooth and mammary gland (Karaplis *et al.*, 1994; Wysolmerski *et al.*, 1998; Philbrick *et al.*, 1998). Consistent with this role, high levels of both the PTHrP and PPR are often expressed within regions of developing organs that are undergoing proliferation or differentiation (Lee *et al.*, 1995; Dunbar *et al.*, 1998; Philbrick *et al.*, 1998). In each of these tissues, high levels of the PPR transcripts are present in mesenchyme-derived cell types such as growth plate chondrocytes, osteoblasts, dental papilla cells and primary mammary mesenchyme fibroblasts, and lack of signaling from this receptor leads to profound disruption in the morphogenesis of these organs (Karaplis *et al.*, 1994; Lee *et al.*, 1995; Dunbar *et al.*, 1998; Philbrick *et al.*, 1998; Wysolmerski *et al.*, 1998). Recently, N-terminal portion of PTHrP has been reported to inhibit angiogenesis-related behaviors of endothelial cells *in vitro*, and overexpression of the peptide reduced tumor vacularization *in vivo* (Bakre *et al.*, 2002). Premature angiogenesis is speculated to be a component of the chondrodystropy associated with the PTHrP and PPR knockout (KO) mice (Bakre *et al.*, 2002).

In the skin, high levels of PTHrP and PPR mRNA transcripts are restricted to the hair follicle and are modulated during the hair cycle. The hair follicle is a mini organ with a complex regenerative growth cycle consisting of three major phases: anagen, catagen, and telogen (Paus and Cotsarelis, 1999). Anagen is the growth phase consisting of the generation of the hair shaft-forming non-permanent portion

[1]*Department of Medical Sciences, Indiana University School of Medicine, Bloomington, Indiana, USA;* [2]*Department of Internal Medicine, Yale University School of Medicine, New Haven, Connecticut, USA;* [3]*Department of Dermatology, Indiana University School of Medicine, Indianapolis, Indiana, USA and* [4]*Institute for Molecular Biology, Indiana University, Bloomington, Indiana, USA*

Correspondence: Dr John Foley, Department of Medical Sciences, Indiana University School of Medicine, Jordan Hall, Bloomington, Indiana 47405, USA. E-mail: jgfoley@indiana.edu

Abbreviations: KO, knockout; KrP, K14-PTHrP; PTH, parathyroid hormone; PTHrP, parathyroid hormone-related protein; PPR, parathyroid hormone (PTH)/parathyroid hormone-related protein (PTHrP) receptor; TSP1, thrombospondin 1; VEGF, vascular endothelial growth factor; wt, wild type

Received 25 January 2006; accepted 22 March 2006; published online 4 May 2006

of the follicle as well as production of the hair shaft. Catagen is a regression phase, where the non-permanent portion undergoes apoptosis and telogen is the resting phase of the cycle. The hair cycle is coordinated by a complex exchange of growth factors/developmental regulatory molecules between the epidermal hair follicle components and dermal papilla/dermal sheath (Millar, 2002). In addition, anagen requires extensive angiogenesis to meet the metabolic needs of the rapidly proliferating cells of the matrix that produce the hair shaft (Mecklenburg *et al.*, 2000). PTHrP mRNA levels decrease in early anagen, and peak during late anagen when much of the outer root sheath of the non-permanent portion of the hair follicle acquires expression of these transcripts (Cho *et al.*, 2003). In contrast to PTHrP transcripts, PPR mRNA is very low in the adult, but peaks during early anagen as transcripts become detectable in the connective tissue sheath that surrounds growing hair follicle (Cho *et al.*, 2003). The location of PTHrP and PPR mRNA suggests that the ligand–receptor pair could participate in the epithelial–mesenchymal interactions that control hair growth.

Several lines of evidence have implicated PTHrP–PPR signaling as a regulator of hair growth. A PPR antagonist (PTH 7–34 amide) injected into neonatal and adult mice appeared to increase the duration of anagen (Holick *et al.*, 1994; Schilli *et al.*, 1997), whereas *in vivo* application of the agonists (PTH 1–34 and PTHrP 1–34) triggered premature catagen (Peters *et al.*, 2001). These findings were supported by the observation that the hair on the dorsal surface of the K14-PTHrP (KrP) mouse is 30–40% shorter and hair follicles enter catagen approximately 2 days early (Cho *et al.*, 2003). Thus, N-terminal PTHrP appears to modulate the hair cycle, but precisely how this signaling affects cellular behavior within the hair follicle has not been elucidated.

In this paper, we use mouse lines that harbor targeted deletions of both PTHrP and PPR along with a series of hair follicle studies on the KrP mice to further define the function of this signaling system within the skin. Here we report that PTHrP overexpression contributes to a shortened hair cycle by reducing proliferation in the matrix during late anagen. Mice that overexpress PTHrP attract less vasculature to the hair follicle. Finding a reciprocal phenotype in the PTHrP and PPR-KO fetuses suggests that this peptide receptor combination is a potent regulator of angiogenesis in the skin.

RESULTS

Overexpression of PTHrP during the adult hair cycle contributes to the short hair phenotype of the KrP mouse

The nipple-like phenotype of ventral skin of the KrP mouse is the result of PTHrP overexpression during a critical window during mammary gland development (Foley *et al.*, 2001). As a result, PTHrP overexpression limited to the adult does not produce nipple-like skin on the ventral surface (Foley *et al.*, 2001). We speculated that the short hair phenotype of the KrP mice might also be the result of the impact of the peptide on the developing hair follicle. We used the previously developed K14-tTA and Tet_o-PTHrP bitransgenic tetracycline-off system (Foley *et al.*, 2001) to control the timing of PTHrP overexpression in the skin. We used three groups of bitransgenic mice and their controls (wild-type (wt) and various single transgenic littermates). The first group of mice was kept on a high dose of tetracycline at all times and this group was considered to be PTHrP-off mice. The second group of mice was kept on a very low dose of tetracycline and this group was considered to be the PTHrP-on mice and it modeled the traditional KrP mouse. The third group of mice were kept on a high dose of tetracycline during development and the first hair cycle. At 16 days after birth (the end of the first hair cycle) the third set was taken off tetracycline, and this group was considered to be the PTHrP-off/on mice. Hair shafts from all groups of mice were harvested at 8 weeks of age when the majority of the pelage would have been replaced during the natural progression through the second hair cycle that occurs after 3 weeks. The various tetracycline-dosing regimens did not alter hair shaft length in the control animals (not shown). The three main types of hair shafts were 18–21% shorter on 8-week-old PTHrP-off mice as compared to controls (Figure 1a). The three main hair types were 23–32% shorter on the 8-week-old PTHrP-on mice as compared to controls and were 7–15% shorter than those from the PTHrP-off mice (Figure 1a). The hair shaft lengths of the 8-week-old PTHrP-off/on were 26–32% shorter than those from control mice and 9–15% shorter than those from PTHrP-off mice (Figure 1a). Consistent with these measures, we found that the majority of zigzag hair shafts from control and PTHrP-off mice clearly had four segments, whereas the fourth

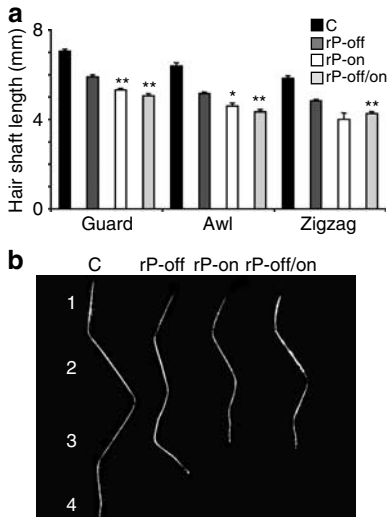

Figure 1. High levels of PTHrP overexpression during the second hair cycle results in shorter hair shafts. (**a**) The graph shows the mean length ± SEM of the three major types of dorsal hairs from wt and single transgenic littermates (C), K14-tTA and Tet_o-PTHrP (bitransgenic) mice on high levels of tetracycline throughout the life (rP-off), bitransgenic mice on low levels of tetracycline throughout life (rP-on), bitransgenic mice on high levels of tetracycline during development as well as the first 16 days post-birth and then taken off the drug for the remainder of the experiment (rP-off/on). Guard, awl, and zigzag hair shaft lengths were found to be shorter in the rP-on and rP-off/on groups than those of the rP-off group (**$P<0.01$), (*$P<0.05$). $N=3$ for all groups except C which was 6. (**b**) Photomicrograph showing zigzag hair shafts from the four groups of mice described above. Note that the hairs from the rP-on and rP-off/on groups lack a distinct fourth segment and the third segment is shorter. Bar = 1 mm.

segment was truncated in the PTHrP-on and PTHrP-off/on mice (Figure 1b). Thus, it appears that induction of high levels of epidermal-derived PTHrP during the second hair cycle in adult mice can produce shorter hair shafts. However, the substantially shorter hair shafts observed in the bitransgenic mice on high doses of tetracycline suggest that this regulated transgene system might be leaky and unsuitable for use in further studies.

Morphometric analysis of the hair growth defect in KrP mice

The original observations establishing that the KrP mice have shorter hair shafts were based largely on measures of telogen hair follicles. We used histomorphometric analysis of hair follicles and measures of both hair shafts in the traditional KrP mice and littermates to determine the point in the hair cycle that is altered by transgene overexpression. Hair follicle lengths of the KrP mice at 6, 9, 12, and 14 days post-depilation were indistinguishable from those of wt littermates (not shown). Prior to the entrance into catagen (day 17 post-depilation for the KrP mice) the length of all three types of hairs shafts from the transgenics are equivalent to that of wt littermates (Figure 2a). Furthermore, the zigzag hairs from transgenic and littermates both had three segments, suggesting that the fourth segment of the wt mice grows after day 17 (Figure 2b). In contrast, although the hair follicle diameters of the KrP and wt littermates were similar at 12 days after depilation, by 14 days the diameter of the transgenic hair bulb was decreased by 23% as compared to wt (Figure 2e). At 12 days post-depilation, hair shaft diameters of the KrP mice were similar to littermates (not shown); however by 17 days post-depilation, hair shaft diameter was decreased 20–30% in the transgenic as compared with wt littermates (Figure 2d). Obvious differences in awl hair shaft diameter were observed at 16 days post-depilation (Figure 2c). Thus, the KrP mice have thinner hair follicles and this defect was apparent during late anagen.

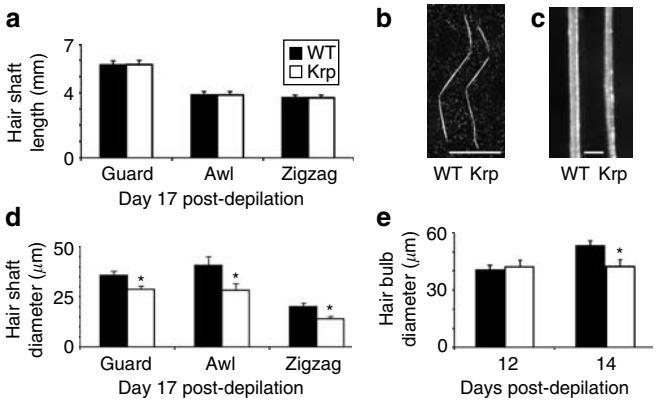

Figure 2. Morphometric evaluation of hair shafts and follicles mice identifies a late anagen defect. (**a**) At day 17 post-depilation, no differences were observed in the hair shaft lengths between wt and KrP mice. The graph shows the mean length ± SEM of the three major types of dorsal hairs $N = 7$ mice in each group. (**b**) Photomicrograph showing zigzag hair shafts from the wt and KrP mice just as the transgenic enters catagen (day 17 post-depilation). Note that both groups have three segments. Bar = 1.33 mm. (**c**) Photomicrograph of proximal region of awl hair shafts at day 17 post-depilation with wt on the left and KrP on right. Bar = 100 μm. (**d**) Mean diameter at the widest portion of the hair shaft (most proximal) ± SEM of three types of dorsal hair form the KrP mice at 17 days post-depilation relative to wt littermates. Guard, awl, and zigzag hair shaft diameters from the KrP mice were found to be 80, 70, and 69% that of wt, respectively (*$P < 0.01$). $N = 7$ mice for each group. (**e**) Mean diameter ± SEM of the hair follicle at the bulb region at days 12 and 14 post-depilation. At day 12 post-depilation, hair bulb diameter of the KrP mice was similar to wt, whereas by day 14 this parameter was decreased by 23% in the transgenics (*$P < 0.01$). $N = 7$ mice in each group.

Proliferation and apoptosis in the KrP mice

Pharmacologic and genetic manipulations that produced shorter hair shafts in mice often are associated with reduced cellular proliferation in the matrix of the hair follicle. BrdU incorporation was used to establish that there was a reduction in the number of proliferating cells in the matrix of the KrP hair follicles during late anagen (Figure 3a and b). During early anagen (days 3–9), the number of proliferating cells in the matrix of the hair follicle were similar in the KrP mice as compared to wt littermates. However, as the hair cycle reached late anagen (days 12–17 for the KrP mouse), the number of

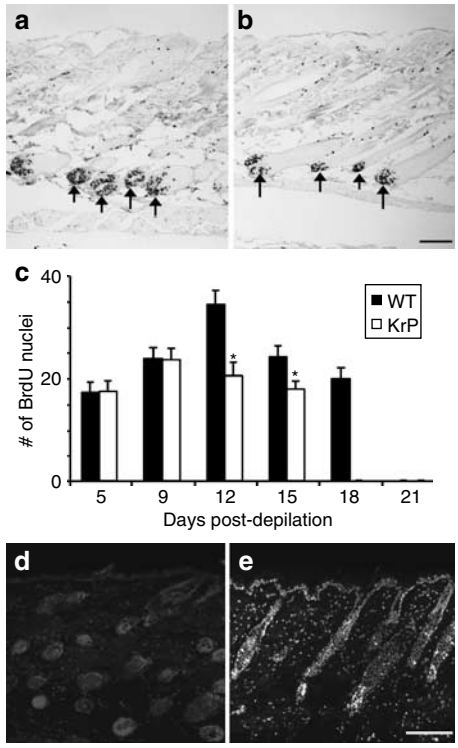

Figure 3. Hair follicle proliferation and cell death in the KrP mice. (**a** and **b**) BrdU-stained sections from formalin-fixed, paraffin-embedded, day 12 post-depilation; (**a**) wt and (**b**) KrP. Arrows indicate matrix region of hair follicle. Bar = 100 μm. (**c**) The panel shows BrdU-labeled cells ± SEM. The staining detected more proliferating cells (days 12 and 15 post-depilation) in wt as compared to transgenic mice. At day 18 post-depilation the transgenic are in the regressing phase of the hair cycle, whereas the wt is still in anagen. At day 21 post-depilation, both genotypes were in the resting phase of the hair cycle and were not labeled (*$P < 0.01$). $N = 3$ mice in each group at each time point. (**d** and **e**) TUNEL was used to evaluate apoptosis in the KrP mice and littermates 17 days post-depilation: (**d**) wt and (**e**) KrP. Note cell death is observed in the outer root sheath and matrix of the KrP hair follicles but not the wt littermates. Bar = 100 μm.

proliferating keratinocytes of the matrix region was decreased (Figure 3c). Reduced cellular proliferation of the matrix would be expected to be associated with decreased shaft diameter.

During catagen, the cells of the non-permanent portion of the hair follicle undergo apoptosis. Apoptosis was evaluated using the TUNEL technique to confirm that the anagen to catagen transition of the KrP mice arrives 2 days earlier than wt littermates (Figure 3d and e). The labeling of the catagen follicles in the KrP mice was similar to those from wt littermates 19 days after depilation (not shown).

Altered vasculature in skins of mice with that overexpress or lack PTHrP or the PPR

Transgenic mice that alter the expression of factors that regulate angiogenesis have been reported to influence hair follicle diameter and the timing of catagen (Yano *et al.*, 2001, 2003). To determine if decreased hair follicle/shaft and premature catagen of the KrP mice was associated with decreased angiogenesis, immunohistochemical staining of endothelial cells was employed using the mAb against CD31 (platelet/endothelial cell adhesion molecule-1) (Horak *et al.*, 1992; Couffinhal *et al.*, 1998) (Figure 4a and b). By histormorphometric analysis, significant decreases in vascular diameter were observed throughout anagen (days 9 and 12) as well as catagen in the KrP mice (day 17) (Figure 5a). No difference in this parameter was observed at telogen (day 21) (Figure 5a). Next, we chose a late anagen time point for the histomorphometric analysis of vascular length. The KrP mice were found to have a 33% decrease in vessel length as compared to wt littermates at 12 days after depilation (not shown). Also, we found an increased distance from the vasculature staining to the hair follicle in the transgenic mice as compared to wt littermates throughout the entire hair cycle (Figure 5b).

To further investigate whether PTHrP as well as the PPR participate in regulation of angiogenesis of the skin, CD-31 staining was performed on PTHrP and PPR-KO skins. Increased vasculature was observed in both the PTHrP and PPR-KO mice as compared to wt littermates (Figure 4c–f). Also, we found increased vessel diameter and length in the PPR and PTHrP-KO mice as compared to wt littermates (Figure 5c and d). Interestingly, increased vasculature was found just below the epidermis in the PTHrP and PPR-KO mice as compared to wt littermates (Figure 5e). Thus, the increased PTHrP expression was correlated with decreased vessels in adult skin, and the lack of PTHrP and the PPR was associated with increased vasculature in fetal skin.

Vascular endothelial growth factor (VEGF) expression has been reported to be a potent regulator of skin angiogenesis as well as a modulator of hair growth (Yano *et al.*, 2001). Long recognized as potent angiogenic factor (Simons, 2004) as well as a gene product controlled by PPR signaling in mesenchymal cells (Hurley *et al.*, 1999), fibroblast growth factor-2 expression has not been studied in relationship to the hair cycle. We wanted to determine if increased PTHrP expression altered the production of these proganigenic factors in murine skin. Western blotting failed to detect differences in VEGF and fibroblast growth factor-2 protein levels in the KrP mice as compared to wt littermates at any point over the course of the hair cycle (Figure 6a and b). In addition, immunohistochemistry and Western blots were performed with thrombospondin 1 (TSP1) and 2 and angiopoiten 1 and 2 antibodies, but no differences in expression of these proteins were observed in KrP mice as compared to littermates (data not shown). These findings suggest that the reduced vasculature in the KrP mice was not accompanied by alterations in the expression of recognized angiogenesis-regulatory factors.

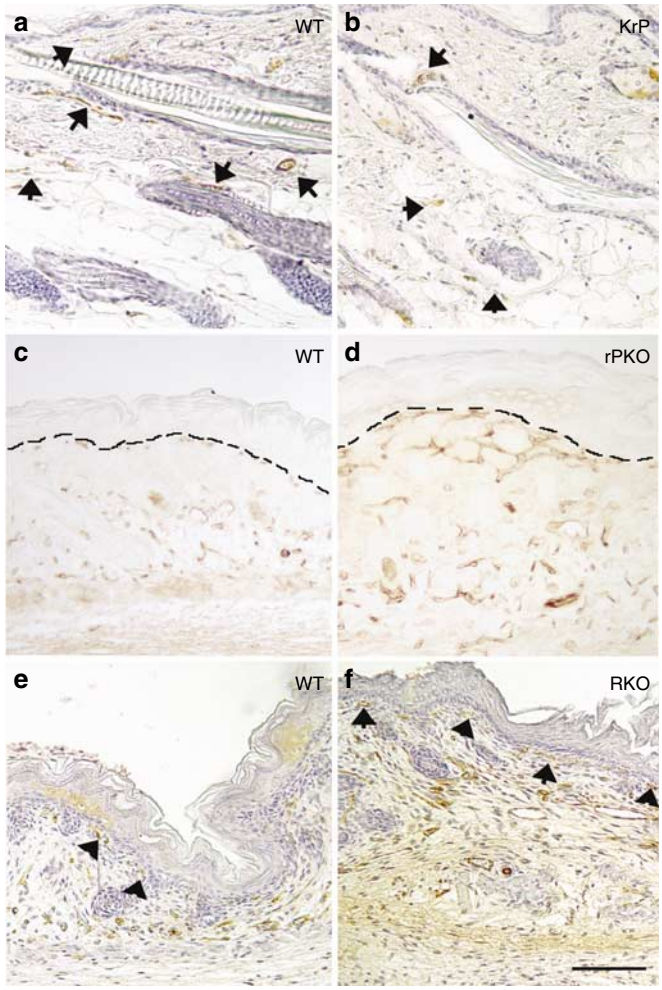

Figure 4. Changes in dermal vasculature observed in mice with altered PTHrP and PPR expression. (**a** and **b**) CD-31 immunostaining of wt and KrP transgenic skins demonstrate diminished perifollicular vessel surrounding anagen follicles in the transgenic samples at day 12 post-depilation. Arrows indicate stained blood vessels. (**c** and **d**) CD-31 immunostaining of E19 WT and PTHrP-KO (rPKO) skins indicate increased vasculature found in the KO samples. Note the increased vasculature is found along the basement membrane (dotted line) of the KO mouse relative to the wt littermate. (**e** and **f**) CD-31 immunostaining of E19 wt (WT) and PPR-KO (RKO) skins demonstrate increased vasculature found in the KO samples. Note the increased vasculature found along the basement membrane of the KO mouse relative to the wt littermate (arrowheads). (**a**–**f**) Bar = 81 μm.

Overexpression of PTHrP reverses delayed catagen in the TSP1-KO mice

Mice that overexpress or lack the antiangiogenic factor TSP1 have alterations in perifollicular vascularization as well as the

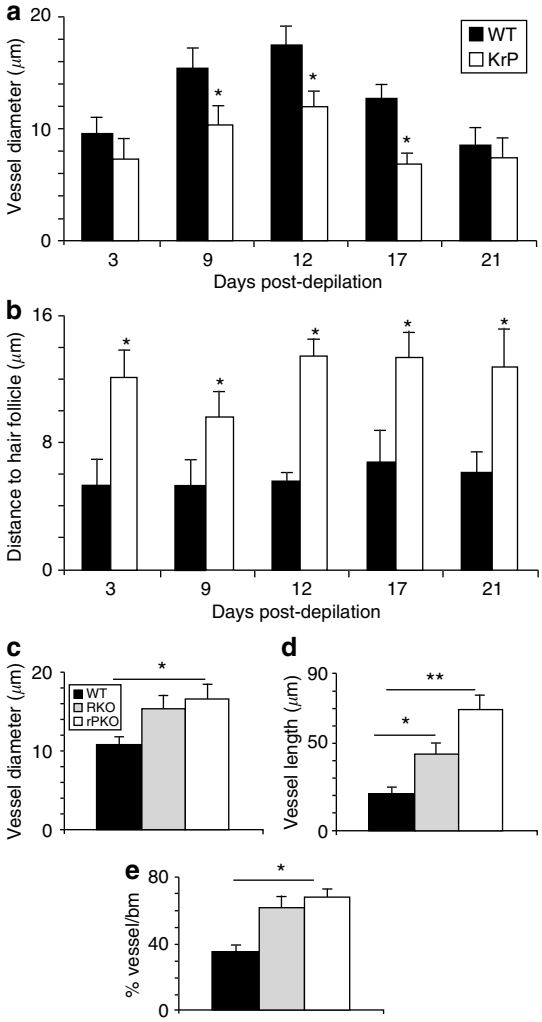

Figure 5. Morphometric analysis of vasculature defects in mice with altered PTHrP and PPR expression. (**a**) Histomorphometric analysis of CD-31-stained vasculature revealed a decrease in mean vessel diameter ± SEM ($P<0.01$) at days 9, 12, and 17 days post-depilation in transgenic mice. $N=5$ samples for each group. (**b**) Histomorphometric analysis of CD-31 stained tissue revealed a significantly increased mean vessel distance from hair follicles ± SEM in the transgenics ($P<0.01$). (**c**) Mean vessel diameter ± SEM of WT, PPR-KO (RKO), and PTHrP-KO (rPKO) mice at embryonic day 19 ($P<0.01$). $N=6$ samples for each genotype. (**d**) Mean vessel length ± SEM of WT, RKO, and rPKO mice at embryonic day 19 ($P<0.01$). (**e**) The ratio derived by measuring vessels adjacent to basement membrane over the total length of the basement membrane ± SEM from WT, RKO, and rPKO mice. The vessels lined a greater fraction of the basement membrane in KOs than was observed in the WT samples ($P<0.01$).

initiation of catagen (Yano *et al.*, 2003). We reasoned that if PTHrP inhibited hair cycle induced angiogenesis, over expression of the peptide might reverse hair cycle defects of the TSP1-KO mice. We crossed the KrP mice with TSP1-KO mice and then crossed the F1 generation, producing KrP/TSP1-KO mice and various littermates. We measured awl hair shafts from mid-dorsum of adult mice 22 days post-depilation and found that the KrP/TSP1-KO hair shaft lengths were similar in length to that of the KrP mice (Figure 7e). TSP1-KO hairs were slightly longer than wt hairs due to

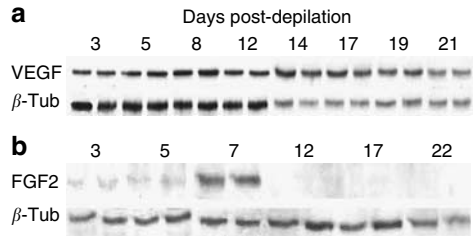

Figure 6. VEGF and β-FGF protein expression levels in the KrP mice were not altered over the course of the hair cycle. (**a**) Western blotting using an anti-VEGF antibody on 15 μg of total protein isolated from the dorsal surface of 8-week-old KrP mice revealed that the VEGF protein levels were unchanged relative to wt littermates. The samples are arranged in pairs of lanes under each number and left is wt and the right KrP. (**b**) Western blotting using anti-β-FGF antibody on blots prepared as above revealed that the β-FGF protein levels were unchanged in the transgenics relative to wt littermates. Samples arranged as above.

catagen being delayed by a day (Yano *et al.*, 2003) (Figure 7e). Next, we measured vascular diameter and length in mice of each genotype 8 days after depilation. Vascular diameter and length of the KrP/TSP1-KO cross at 8 days post-depilation were similar to those of the KrP mouse (not shown). At the time point when the KrP mice enter catagen (day 17 post-depilation), the TSP1-KO skin had increased CD31 staining relative to wt littermates (Figure 7a and b), but the vasculature labeling in the KrP/TSP1-KO was indistinguishable from that of KrP mice (Figure 7c and d). Thus, the overexpression of PTHrP reverses the vascular changes and delayed catagen observed in the TSP1-KO mouse.

DISCUSSION

The growth of new capillaries from pre-existing blood vessels during the hair cycle is one of the few non-pathological circumstances in which angiogenesis occurs in adult mammals (Mecklenburg *et al.*, 2000). The study of the molecular regulation of angiogenesis of the hair follicle is in its initial stages. However, a series of mouse studies focusing on the proangiogenesic factor VEGF and the antiangiogenesis factor TSP1 serve as benchmarks for gene expression changes and action of angiogenesis-regulatory molecules in the context of the hair cycle. VEGF is a secreted protein that serves as a mitogen for endothelial cells and induces vascular hyperpermeability (Carmeliet, 2005), whereas TSP1 is an extracellular matrix-associated glycoprotein that inhibits angiogenesis by an unknown mechanism (Bornstein, 2001). From a series of studies by Detmar and colleagues, it appears that alterations in growth factors and matrix that promote angiogenesis in the skin would be expected to lead to an increased hair growth rate as well as thicker and longer hair shafts (Yano *et al.*, 2001, 2003). Conditions that result in reduced angiogenesis would lead to a decreased growth rate resulting in shorter and thinner hair shafts (Yano *et al.*, 2001, 2003). Moreover, decreased angiogenesis is thought to underlie the miniaturization of the hair follicle that characterizes androgenic alopecia (Cormia and Ernyeye, 1961).

The expression pattern of PTHrP and its impact on hair growth suggest a role as an angiogenesis inhibitor. PTHrP

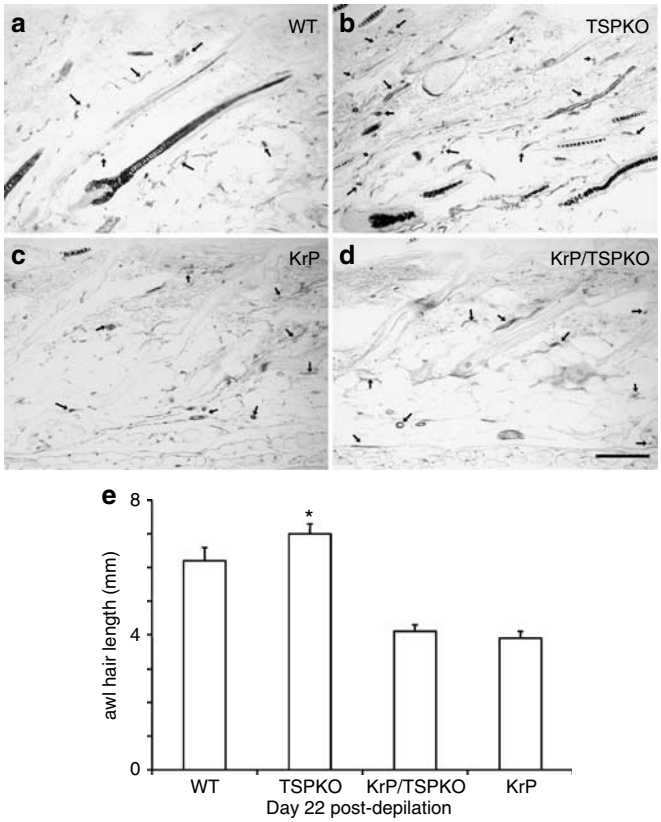

Figure 7. Overexpression of PTHrP reverses the delayed catagen of the TSP1-KO mouse. (**a**–**d**) CD-31 immunostaining of (**a**) WT, (**b**) TSP1-KO, (**c**) KrP, and (**d**) KrP/TSP1-KO mice at 17 days post-depilation. KrP/TSP1-KO mice did not have increased vasculature relative to the KrP mice, whereas the TSP1-KO skin exhibited increased CD31 stain as compared to WT. Arrows indicate stained blood vessels. Bar = 50 μm. (**e**) The mean awl hair shaft lengths ± SEM of dorsal hair from WT, TSP1-KO, KrP/TSP1-KO, and KrP mice at 22 days post-depilation. Note that both the KrP and KrP/TSP1-KO mice have shorter awl hair shaft lengths as compared to wt and TSP1-KO mice. $N = 3$ mice of each genotype. $P < 0.05$ between TSP1-KO hair shafts relative to WT.

levels are very low during early anagen but reach high levels in anagen VI (Cho *et al.*, 2003). The proangiogenic factors VEGF and fibroblast growth factor-2 reached highest levels in early anagen, 3 days prior to the increase in skin vasculature (Yano *et al.*, 2001) (Figure 6). In contrast, the angiogenesis inhibitor TSP1 transcripts peaked during catagen (Yano *et al.*, 2003). Similar to VEGF antibody-treated mice and K14-TSP1 mice, the diameter and length of vessels in the skin of the KrP mice was reduced during late anagen compared to controls (Figure 5). Moreover, the fetal skin of the PTHrP and PPR-KO mice showed increases in these vascular parameters at a time when hair follicle morphogenesis shares some aspects with early anagen (Paus and Cotsarelis, 1999). Interestingly, reduced vessel diameter in the KrP mouse as compared to controls could be statistically established at 9 days post-depilation preceding diminished proliferation of the matrix at 12 days and decreased hair follicle diameter at 14 days. The overexpression of TSP1 or treatments of mice with VEGF antibodies or the angiogenesis inhibitor TNP-470 delays the emergence of hair shafts after depilation (Mecklenburg *et al.*, 2000). This delay was not observed in depilated KrP mice; however, in neonatal mice bearing this transgene as well as those with hair loss induced by chemotherpeutic agents, hair shaft emergence was delayed. (Wysolmerski *et al.*, 1994) (C. Offutt, J. Foley unpublished observation). The reduced hair shaft length observed in the KrP mice appeared to result from premature catagen. In the TSP1-KO mice catagen was delayed by at least 1 day (Yano *et al.*, 2003); however, only modestly longer hair shafts were produced (Figure 7). Given the minimal effect that the lack of TSP1 has on hair shaft length, it was not surprising that lack of this matricellular protein could not reverse the premature catagen triggered by PTHrP overexpression. The lack of alterations in proangiogenic factor expression in the KrP mice suggest that the peptide receptor pair may directly affect endothelial cells within the skin. Consistent with this notion, the application of N-terminal fragments of PTHrP *in vitro* reduced endothelial cell migration on various substrates and triggered apoptosis of proliferating endothelial cells and this was attributed to activation of protein kinase A (Bakre *et al.*, 2002). Taken together, it appears that PTHrP–PPR-mediated inhibition of angiogenesis during the hair cycle could account for some of the peptide's effect on hair growth. Therefore, antagonists and agonists to the PPR may represent potential therapeutics for adult hair cycle disorders or other skin diseases with angiogenesis-dependent components.

MATERIALS AND METHODS

Mice

All experiments that used animals were approved by the Indiana University IACUC and were performed in compliance with stipulations of that body. PTHrP and PPR-KO mice were maintained on a CD-1 background. The KrP transgenic line was also maintained by continued breeding against a CD-1 background.

Six litters of K14-tTA/TetO-PTHrP double transgenic mice were created by crossing K14-tTA transgenic mice with TetO-PTHrP transgenic mice as previously reported in Foley *et al.* (2001). Two sets of litters were kept on 150 mg/ml tetracycline hydrochloride in the water during development and the entire post-natal life and represent the transgene off group. Two litters were placed on a minimal dose of tetracycline hydrochloride (15 mg/ml) that permitted expression of the transgene both during development and postnatal life but prevented neonatal lethality from excessive PTHrP expression during development, and these represent the transgene on group. Two litters were placed on 150 mg/ml tetracycline hydrochloride during development and up to 16 days after birth at which point they were weaned. After weaning these animals were not exposed to tetracycline, which has been shown to activate the transgene and these represent the transgene off/on group (Foley *et al.*, 2001). All bitransgenic mice were harvested when 8-week old.

The TSP1-KO mice were originally on a C57BL/6 background (Lawler *et al.*, 1998). TSP1-KO mice were crossed with KrP transgenic line and were identified by lack of hair on the ventral surface of the KrP mice and by PCR analysis of DNA isolated from tail biopsies for identification of the TSP1-KO mice. The PCR primer sequences were as follows: reverse TSP1 primer

(5′-GAGTTTGCTTGTGGTGAACGCTCAG-3′) and a forward neo primer (5′-TGCTGTCCATCTGCACGAGACTAG-3′) for the mutant allele or a forward TSP1 primer (5′-AGGGCTATGTGGAATTAA TATCGG-3′) for the wt allele. The wt and mutant alleles yield PCR products of 700 and 400 bp, respectively. KrP/TSP1 +/− and TSP +/ −F1 mice were crossed to generate KrP/TSP1 −/− and these were compared to wt, KrP/Tsp +/+, and Tsp−/− littermates.

Hair measurements

Tufts of hair from the mid-dorsum of sex- and color-matched wt and KrP littermates were harvested with a forceps by gently pulling with the orientation of the follicles. Images of hair were digitally captured using a spot RT camera and a Leica dissecting scope. The length of individual hairs was measured using an image analysis program (ImageJ). Ten to fifty hairs of each type were measured from 3 to 7 mice of every genotype and age; however, only male mice were used. Results were expressed as a mean ± SEM and the two-tailed Student's *t*-test was employed as a test of significance.

Tissue harvesting

To compare the hair cycle of the transgenic mice that overexpress PTHrP with their wt littermates, 8-week-old male mice were depilated using a wax-rosin hair remover. Skin samples were harvested at various time points to get representative samples of cycling hair on various days post-depilation. Experiments using the KrP mice crossed with the homozygous TSP1-KO mice were compared with the same KrP (TSP intact) as well as TSP1-KO littermates. Dorsal tissue samples were collected 8 and 17 days after depilation of these 8-week-old transgenic mice. The experiments were repeated three times. For the hair cycle analysis at least three and up to seven mice at each time point and each genotype were evaluated.

Histology and immunohistochemistry

Skin samples (1–2 cm^2) were removed from the mid-dorsum and fixed directly in 10% buffered formalin or zinc fixative (Pharmingen, San Diego, CA). Tissues were dehydrated, embedded in paraffin, and 6 μm sections were cut. A monoclonal rat anti-CD31 (Pharmingen, San Diego, CA), rabbit polyclonal antibodies to TSP1 and TSP-2 (Abcam, Cambridge, MA) were used with a procedure similar to that in Foley *et al.* (2001). Immunohistochemistry and histology was performed on multiple skin sections from three to seven mice of each genotype and age.

Western blotting

Skin samples (1 cm^2) were removed from the mid-dorsum and snap frozen in liquid nitrogen before being placed in –80°C freezer until further use. Each sample was then ground into a fine powder by mortar and pestle while immersed in liquid nitrogen before being poured into a 7 ml plastic scintillation vial containing 1 ml RIPA buffer (150 mM NaCl, 10 mM Tris, pH 7.2, 0.1% SDS, 1.0% Triton X-100, 1% deoxycholate, 5 mM EDTA with the protease inhibitors of 1 mM phenylmethylsulfonyl fluoride, 5 μg/ml leupeptin, 5 μg/ml pepstatin, and 5 μg/ml aprotinin). Samples were then homogenized before being microcentrifuged at 4°C at 13,000 r.p.m. for 5 minutes. Supernatant was then isolated and centrifuged again. Normalization of protein was carried out by BCA kit (bioRad, Hercules, CA). In all, 20 μl of 1 μg/μl of protein was combined with 10 μl of 3 × Laemlli sample buffer and then boiled for 5 minutes before subsequently loaded onto 8% Laemlli polyacrylamide gels. Running the gels and blotting was performed as in Foley *et al.* (2000). The efficiency of transfer was assessed by incubating the blotted gel in 0.1% Coomassie brilliant blue for 1 hour followed by 30 minutes in destaining solution. The following polyclonal antibodies were used: (rabbit anti-VEGF 147 (1/1,000) and rabbit anti-fibroblast growth factor-2 H-131 (1/500), goat antiangiopoiten 1 N-18 (1/200), and goat antiangiopoiten 1 E-18 (1/200; Santa Cruz). Blots were stripped and reprobed with a monoclonal to β-tubulin 6B1 (1/1,000 Santa Cruz Biotechnology, Santa Cruz, CA). These experiments were repeated twice so that immunoreactivity from two mice of each genotype and time point was evaluated.

Computer-assisted morphometric vascular analysis

Immumohistochemical staining of 6 μm sections of blood vessels using the mAb CD31 were analyzed using a Nikon E-400 microscope (Nikon, Melville, NY). Images were captured with a Spot digital camera (Diagnostic Instruments, Sterling Heights, MI) and morphometric analyses were performed using ImageJ software (NIH). At least seven different fields of each section of at least three mice per time point were examined at × 20 magnification with the microscope and further magnification of the recorded image with ImageJ to × 80. The average vessel length, diameter, and distance from the hair follicle were assessed. The two-sided unpaired *t*-test was used to establish significance.

BrdU incorporation/TUNEL

Mice were injected intraperitoneally with BrdU (Sigma-Aldrich, St Louis, MO) dissolved in PBS (20 μg/g body weight) 2 hours before killing. Harvested tissue was fixed in 10% formalin fixative and embedded in paraffin. BrdU was examined immunohistochemically using anti-BrdU antibody (Developmental Studies Hybridoma Bank, University of Iowa, Iowa City, IA) and peroxidase-labeled secondary antibody and developed using 3,3′-diaminobenzidine tetrahydrochloride. Multiple skin sections from at least three mice were evaluated for each time point. Counts were restricted to the matrix of the growing hair follicles. TUNEL was performed with the Programmed Cell Death Kit (Roche, Indianapolis, IN), using formalin-fixed, paraffin-embedded tissue according to the manufacturer's instructions.

CONFLICT OF INTEREST

The authors state no conflict of interest.

ACKNOWLEDGMENTS

A special thanks to Sue Childress for her prompt and professional histological technical support. Also, Todd Gocken is thanked for providing technical expertise. This work was supported by National Institutes of Health Grant R01 AR45585. Anti-BrdU antibody was provided by Developmental Studies Hybridoma Bank, University of Iowa, Iowa City, IA. We also express our gratitude to Drs Jack Lawler (Harvard Medical School) and Henry Kronenberg (Massachusetts General Hospital) for providing the TSP1-KO, PPR, and PTHrP-KO mice

REFERENCES

Bakre MM, Zhu Y, Yin H, Burton DW, Terkeltaub R, Deftos LJ *et al.* (2002) Parathyroid hormone-related peptide is a naturally occurring, protein kinase A-dependent angiogenesis inhibitor. *Nat Med* 8:995–1003

Bornstein P (2001) Thrombospondins as matricellular modulators of cell function. *J Clin Invest* 107:929–34

Carmeliet P (2005) Angiogenesis in life, disease and medicine. *Nature* 438:932–6

Cho YM, Woodard GL, Dunbar M, Gocken T, Jimenez JA, Foley J (2003) Hair-cycle-dependent expression of parathyroid hormone-related protein and its type I receptor: evidence for regulation at the anagen to catagen transition. *J Invest Dermatol* 120:715–27

Cormia F, Ernyeye A (1961) Circulatory changes in alopecia. *Arch Dermatol* 84:772

Couffinhal T, Silver M, Zheng LP, Kearney M, Witzenbichler B, Isner JM (1998) Mouse model of angiogenesis. *Am J Pathol* 152:1667–79

Dunbar ME, Young P, Zhang JP, McCaughern-Carucci J, Lanske B, Orloff JJ *et al.* (1998) Stromal cells are critical targets in the regulation of mammary ductal morphogenesis by parathyroid hormone-related protein. *Dev Biol* 203:75–89

Firkin F, Seymour JF, Watson AM, Grill V, Martin TJ (1996) Parathyroid hormone-related protein in hypercalcaemia associated with haematological malignancy. *Br J Haematol* 94:486–92

Foley J, Dann P, Hong J, Cosgrove J, Dreyer B, Rimm D *et al.* (2001) Parathyroid hormone-related protein maintains mammary epithelial fate and triggers nipple skin differentiation during embryonic breast development. *Development* 128:513–25

Foley J, King CS, Jimenez JA, Wysolmerski JJ, Philbrick WM (2000) Activation of PTHrP gene expression in squamous carcinoma cell lines by mutant isoforms of the tumor suppressor p53. *Oncol Res* 12:71–81

Gardella TJ, Juppner H (2001) Molecular properties of the PTH/PTHrP receptor. *Trends Endocrinol Metab* 12:210–7

Holick MF, Ray S, Chen TC, Tian X, Persons KS (1994) A parathyroid hormone antagonist stimulates epidermal proliferation and hair growth in mice. *Proc Natl Acad Sci USA* 91:8014–6

Horak ER, Leek R, Klenk N, LeJeune S, Smith K, Stuart N *et al.* (1992) Angiogenesis, assessed by platelet/endothelial cell adhesion molecule antibodies, as indicator of node metastases and survival in breast cancer. *Lancet* 340:1120–4

Hurley MM, Tetradis S, Huang YF, Hock J, Kream BE, Raisz LG *et al.* (1999) Parathyroid hormone regulates the expression of fibroblast growth factor-2 mRNA and fibroblast growth factor receptor mRNA in osteoblastic cells. *J Bone Miner Res* 14:776–83

Karaplis AC, Luz A, Glowacki J, Bronson RT, Tybulewicz VL, Kronenberg HM *et al.* (1994) Lethal skeletal dysplasia from targeted disruption of the parathyroid hormone-related peptide gene. *Genes Dev* 8:277–89

Lawler J, Sunday M, Thibert V, Duquette M, George EL, Rayburn H *et al.* (1998) Thrombospondin-1 is required for normal murine pulmonary homeostasis and its absence causes pneumonia. *J Clin Invest* 101:982–92

Lee K, Deeds JD, Segre GV (1995) Expression of parathyroid hormone-related peptide and its receptor messenger ribonucleic acids during fetal development of rats. *Endocrinology* 136:453–63

Mecklenburg L, Tobin DJ, Muller-Rover S, Handjiski B, Wendt G, Peters EM *et al.* (2000) Active hair growth (anagen) is associated with angiogenesis. *J Invest Dermatol* 114:909–16

Millar SE (2002) Molecular mechanisms regulating hair follicle development. *J Invest Dermatol* 118:216–25

Paus R, Cotsarelis G (1999) The biology of hair follicles. *N Engl J Med* 341:491–7

Peters EM, Foitzik K, Paus R, Ray S, Holick MF (2001) A new strategy for modulating chemotherapy-induced alopecia, using PTH/PTHrP receptor agonist and antagonist. *J Invest Dermatol* 117:173–8

Philbrick WM, Dreyer BE, Nakchbandi IA, Karaplis AC (1998) Parathyroid hormone-related protein is required for tooth eruption. *Proc Natl Acad Sci USA* 95:11846–51

Schilli MB, Ray S, Paus R, Obi-Tabot E, Holick MF (1997) Control of hair growth with parathyroid hormone (7–34). *J Invest Dermatol* 108:928–32

Simons M (2004) Integrative signaling in angiogenesis. *Mol Cell Biochem* 264:99–102

Wysolmerski JJ, Broadus AE, Zhou J, Fuchs E, Milstone LM, Philbrick WM (1994) Overexpression of parathyroid hormone-related protein in the skin of transgenic mice interferes with hair follicle development. *Proc Natl Acad Sci USA* 91:1133–7

Wysolmerski JJ, Philbrick WM, Dunbar ME, Lanske B, Kronenberg H, Broadus AE (1998) Rescue of the parathyroid hormone-related protein knockout mouse demonstrates that parathyroid hormone-related protein is essential for mammary gland development. *Development* 125:1285–94

Yano K, Brown LF, Detmar M (2001) Control of hair growth and follicle size by VEGF-mediated angiogenesis. *J Clin Invest* 107:409–17

Yano K, Brown LF, Lawler J, Miyakawa T, Detmar M (2003) Thrombospondin-1 plays a critical role in the induction of hair follicle involution and vascular regression during the catagen phase. *J Invest Dermatol* 120:14–9